Unified Picture for the Colossal Thermopower Compound $FeSb_2$

M. Battiato,* J. M. Tomczak, Z. Zhong, and K. Held
Institute for Solid State Physics, Vienna University of Technology, Vienna A-1040, Austria
(Received 20 January 2015; published 10 June 2015)

We identify the driving mechanism of the gigantic Seebeck coefficient in $FeSb_2$ as the phonon-drag effect associated with an in-gap density of states that we demonstrate to derive from excess iron. We accurately model electronic and thermoelectric transport coefficients and explain the so far ill-understood correlation of maxima and inflection points in different response functions. Our scenario has far-reaching consequences for attempts to harvest the spectacular power factor of $FeSb_2$.

DOI: 10.1103/PhysRevLett.114.236603 PACS numbers: 72.20.Pa, 71.20.-b, 71.27.+a

Introduction.—Thermoelectrics [1] hold great promise for sustainable energy solutions [2] and technological applications such as Peltier coolers, heat pumps [3], microscopic generators [4], and probes for quality control of solid state devices [5]. In recent years, more and more intermetallic compounds with narrow gaps have been found to exhibit large thermoelectrical effects. Among them, the iron antimonide $FeSb_2$ [6–9] is the most prominent. In fact, it boasts the largest thermoelectric power factor ever measured [8–11]. The thermopower assumes its maximum at around 15 K, making $FeSb_2$ the prime candidate for thermoelectric cooling devices at cryogenic temperatures. The origin of the large thermoelectrical response is, however, unknown to date. While electronic correlation effects have been advocated as a main benefactor [7–14], other works suggested the so-called phonon-drag effect to cause the colossal thermopower [15,16].

Besides the large magnitude of thermoelectricity, several transport quantities of $FeSb_2$ exhibit a pronounced temperature dependence [8–14]. In particular, there is a correlation of features in different response functions [12,14,17]: Extrema in the Nernst coefficient correspond to inflection points in both the Seebeck coefficient and the resistivity. Likewise, at these characteristic temperatures features appear in the magnetoresistance and the Hall coefficient. This intimate linkage between electrical and thermoelectrical quantities heralds a connection to the mechanism behind the colossal Seebeck effect. Yet, in all, so far no convincing comprehensive physical picture for this distinctive behavior has been proposed.

Here, we unveil the origin behind the characteristic temperature scales, as well as the mechanism for the colossal thermoelectricity in $FeSb_2$. We report a minimal model consisting of an effective one-particle electronic structure with two crucial ingredients: (i) narrow in-gap states and (ii) an electron-phonon coupling mechanism. Our approach captures all transport phenomena on a quantitative level and pinpoints a new scenario for thermoelectricity in $FeSb_2$, from which the phonon-drag associated with an in-gap density of states emerges as the main driver. Finally, using first principles calculations, we identify a diminutive (intrinsic) off-stoichiometry, $Fe_{1+x}Sb_{2-x}$, as the likely origin of these in-gap states, in line with the large sample dependence of experimental observables possibly due to different crystal growth techniques [6–14].

Theoretical framework.—Employing Boltzmann's theory in the relaxation time approximation [18], we study a variety of electrical and thermoelectrical observables. For the latter, we explicitly include contributions from the phonon-drag effect: A thermal gradient $\nabla_{\mathbf{r}}T$ produces an out-of-equilibrium population in the phonon Brillouin zone. In the case of acoustic phonons, at low temperature the effect is an increase in the population for wave vectors opposite the direction of the thermal gradient. This will induce a heat flux. However, scatterings will drive this phonon population back towards thermal equilibrium. One mechanism responsible for the latter is the scattering with electrons, a process in which linear momentum is transferred to the electronic subsystem: the phonon-drag effect. The correct, yet cumbersome, way to treat these scattering events is to add a term to the collision integral in the Boltzmann equation. Instead, we here propose, as an elegant short cut, to treat the discrete scatterings as a continuous injection of linear momentum. It is easy to show that for isotropic acoustic phonon branches, the transferred linear momentum is proportional to $\nabla_{\mathbf{r}}T$. Thus, an effective description of the phonon drag is achieved by adding a term $\propto \nabla_{\mathbf{r}}T$ to the semiclassical equation of motion of the electrons

$$\dot{\mathbf{k}} = -\frac{e}{\hbar}[\mathbf{E} + \dot{\mathbf{r}} \times \mathbf{B}] - \alpha \nabla_{\mathbf{r}} T, \tag{1}$$

which states that the time derivative of the electron wave vector $\mathbf{k}$ is due to the sum of the external electrical $\mathbf{E}$ and magnetic $\mathbf{B}$ fields, and the contribution from the phonon drag ($\hbar$ is the reduced Planck constant, e the electron's charge, and $\mathbf{r}$ its position at time t satisfying $\dot{\mathbf{r}} = (1/\hbar)\nabla_{\mathbf{k}}\mathcal{E}_i(\mathbf{k})$, where $\mathcal{E}_i$ is the energy dispersion of the ith band). For simplicity, we shall use a band and momentum averaged phonon coupling α. Then, the expressions for the phonon-drag driven Seebeck and Nernst coefficient can be readily computed. For instance,

$$S_{\mathrm{ph}} = \frac{e\alpha}{(2\pi)^3 \hbar \sigma_{zz}} \sum_i N_i \tau_i \int \frac{\partial f}{\partial \mathcal{E}} \left(\frac{\partial \mathcal{E}_i}{\partial k_z} \right)^2 d^3\mathbf{k}, \quad (2)$$

where f is the Fermi function, τ_i the relaxation time, N_i the band degeneracy, and σ the total conductivity.

Evaluating the transport functions requires the knowledge of the dispersions $\mathcal{E}_i$. We choose parabolic conduction and valence bands with equal mass. However, the latter are not enough for a complete description. Comparing the experimental resistivity of $FeSb_2$ to the activated behavior of a perfect semiconductor (see Supplemental Material [18]), we notice that the shoulder around 10 K is a clear fingerprint of defect states inside the gap (as also reported in Refs. [8,10,31]). We therefore explicitly include in-gap states in our treatment and consider, as a practical approximation, pairs of spherically symmetric dispersions: $\mathcal{E}_i^{\pm}(k) = E_i \pm W_i/2 \cos(\pi k/2\tilde{k})$, where the reciprocal lattice vector k lies in a Brillouin zone of radius $\tilde{k}$ and E_i is the energy position and W_i the width of the band.

In the following, it will be important to distinguish between the *temperature dependence* and the *amplitude* of the response functions. It can be proven [18] that each of the transport properties can be expressed by an amplitude factor and a function η that contains all nontrivial temperature dependence. For example, the contribution to the phonon-drag thermopower of an in-gap state can be written as

$$S_{\mathrm{ph}} = \frac{\alpha W_i^2 \tilde{k}_i e \tau_i N_i}{192 \hbar^2 \sigma k_B T} \eta_{S_{\mathrm{ph}}} \left(\frac{E_i - \mu(T)}{k_B T}, \frac{W_i}{2 k_B T} \right). \quad (3)$$

Similar expressions hold for all transport properties, with different amplitude prefactors (depending on W_i, N_i, τ_i, $\tilde{k}_i$) and characteristic η *functions* that all depend on the same two variables: $[E_i - \mu(T)]/k_B T$ and $W_i/2k_B T$. The η functions can be classified into two categories according to their symmetry with respect to their first argument. For example, the conductivity, which does not distinguish between electrons and holes, will have the same amplitude whether the chemical potential is above or below the band center; hence, η_σ is *even*. Conversely, the Hall coefficient has to change sign when the chemical potential is at the band center; η_{R_H} is *odd* in its first argument. The category of an η function thus reflects the sensitivity of the transport property to the type of carriers. A full description can be found in the Supplemental Material [18], while a quick reference is reported in Table I. It is remarkable that while the electronic Seebeck coefficient is sensitive to the carrier type, the phonon-drag driven one is not. As a consequence the relative symmetry between S, N, R_H, and σ can be used to distinguish purely electronic from phonon-drag driven thermoelectricity. Interestingly, we also find that all η functions are only slowly varying with their second argument. In particular, the qualitative shape and the symmetry are inert, and even the peak widths are only weakly dependent on $W_i/2k_B T$. Consequently, the temperature profile of all the transport properties deriving from in-gap states is *entirely* determined by the position E_i of the band with respect to the chemical potential and the absolute temperature. All other parameters merely rescale the *amplitude* in a T-independent fashion.

TABLE I. Schematic representation of the even or odd character of the η functions for in-gap state derived transport.

η-function	σ	R_H	S	N	MR
electronic					
phonon-drag	N/A	N/A			N/A

Temperature dependence of transport properties.—We now allow for one state $\mathcal{E}_1^{\pm}(k)$ inside the charge gap, $\Delta = 30$ meV, to account for the shoulder in the conductivity [we find that $E_1 = 24.3$ meV yields good agreement; see Fig. 1(a)]. All other parameters (W_i, N_i, $\cdots$) merely describe the relative amplitudes for the conduction or valence and in-gap state contributions, and will be discussed later. Here, we first focus on the temperature dependence of the thermoelectric response to elucidate the ill-understood correlations between features in different transport quantities of $FeSb_2$. We consider three scenarios: (i) a purely electronic description of thermoelectricity (with contributions from the VB, CB, and in-gap states), (ii) a dominant phonon-drag effect on valence and conduction carriers, and (iii) a preponderant phonon-drag effect that couples to electronic in-gap excitations. Scenario (i) is known to be insufficient to account for the amplitude of thermoelectricity in $FeSb_2$ [15], but it also yields the wrong temperature profile. Scenarios (i) and (ii) are dominated by valence and conduction contributions so that the Seebeck and the Nernst coefficient have a very comparable temperature dependence and peak positions—-at variance with experiments. For details of the hence discarded scenarios see the Supplemental Material [18].

This leaves us with scenario (iii), a preponderant phonon-drag effect linked to in-gap states, which we advocate in the following. In this picture, the shapes of all transport functions are uniquely determined by a single parameter: the position E_1 of the in-gap state [see the discussion of Eq. (3)]. As can be seen in Fig. 1, this setup correctly predicts the characteristic peak temperature, as well as the line shapes of the major feature in all five transport functions.

The good agreement notwithstanding, there are deviations above 15 K. To understand this issue, we scrutinize the experimental magnetoresistance (MR). We notice that $FeSb_2$ displays a strong response to a magnetic field only in the temperature range where our in-gap band gives a contribution to the conductivity; see Fig. 1. We do not provide an expression for the unconventional linear-in-B MR of this material, as the underlying mechanism is unresolved. Nonetheless, we can argue that the MR cannot distinguish between electron and hole transport and has an even-type η function. Consequently, the MR peaks at the

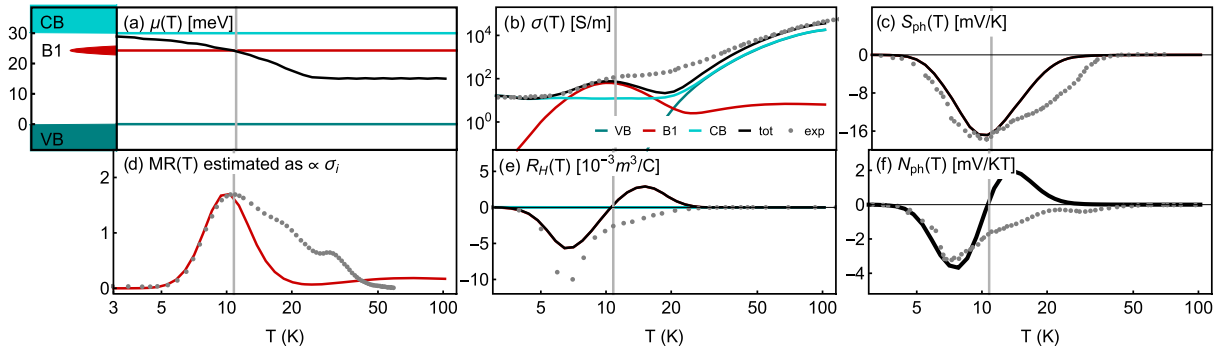

FIG. 1 (color online). Modeled transport properties of $FeSb_2$ with one in-gap state compared to experiment [14]. (a) Density of states (left) and chemical potential μ as a function of temperature (right). (b) Electrical conductivity σ on a logarithmic scale, consisting of valence (VB), conduction (CB), and in-gap band (B1) contributions. (c) Seebeck coefficient, (d) magnetoresistance (MR), (e) Hall coefficient R_H, and (f) Nernst coefficient. The (gray) vertical line indicates the temperature at which the chemical potential passes the in-gap state E_1.

same temperature as the conductivity (the peak width might be different). In Fig. 1(d) we therefore compare the MR to the in-gap-state conductivity and immediately notice that one in-gap band gives only one peak in the MR. However, in the experimental data there are in total three features. In Fig. 2, we therefore refine our model to include three in-gap states (note that a single state with an energy differentiation of its density of states or group velocities can play the same role). All peaks and their correlation in different transport functions are then captured with only three parameters: the energy positions E_i of the in-gap states. To account for relative *amplitudes* (see below), our model includes two further parameters that we extract from the ratios of the Nernst coefficient peak amplitudes. Then, all five transport coefficients follow accurately: In Fig. 2 the peak positions and linewidths of all features are captured [32]. This pinpoints the preponderant influence of in-gap states and their role in the phonon-drag picture as the main driver for the physics of $FeSb_2$.

Amplitude of transport coefficients.—While we focused so far on the temperature profile of transport coefficients, the modeling in Fig. 2 also neatly accounts for the individual amplitudes. We now detail the parameters that quantitatively determine the response functions. The phonon-drag constant can be extracted completely from experiments as $\alpha \approx 3 \times 10^{13}\ \mathrm{s^{-1}\,K^{-1}} = 229.2 k_B/\hbar$ at $T = 10$ K [18].

Since the temperature dependence of the transport functions is uniquely controlled by the positions of the in-gap states, every transport coefficient only contributes one independent value for the determination of the band parameters, W_i, N_i, τ_i. We are thus dealing with a largely underdetermined set of equations. Therefore, we fix some of the parameters of our model to physically reasonable values and then check all remaining adjustable parameters for consistency: We know that N_i has to be of the order of unity, so we assign $N_i = 1$ for all the in-gap bands. Then, the width of the Brillouin zone for in-gap states (we assume $\tilde{k}_{1,2,3} = \tilde{k}$) can be extracted from the ratio of the peak amplitudes of the Nernst and Seebeck coefficient, yielding $\tilde{k} \approx 10^{-2}$ Å^{-1}. Comparing $\tilde{k}$ to the size of the Brillouin zone of perfect $FeSb_2$, we deduce an effective defect concentration of 9×10^{-5}/unit cell. Next, we set $\tau_i = \tau_{\mathrm{CB}} = \tau_{\mathrm{VB}} = 0.3$ ps. This fully determines the in-gap bandwidths for which we find $W_1 = 3$ meV, $W_2 = 4.1$ meV and $W_3 = 5.1$ meV [33].

With all parameters thus fixed, we now check if the value of α is realistic. To this end we compare the linear momentum that is transferred from the phonons to the electrons with that dissipated by lattice thermal conduction.

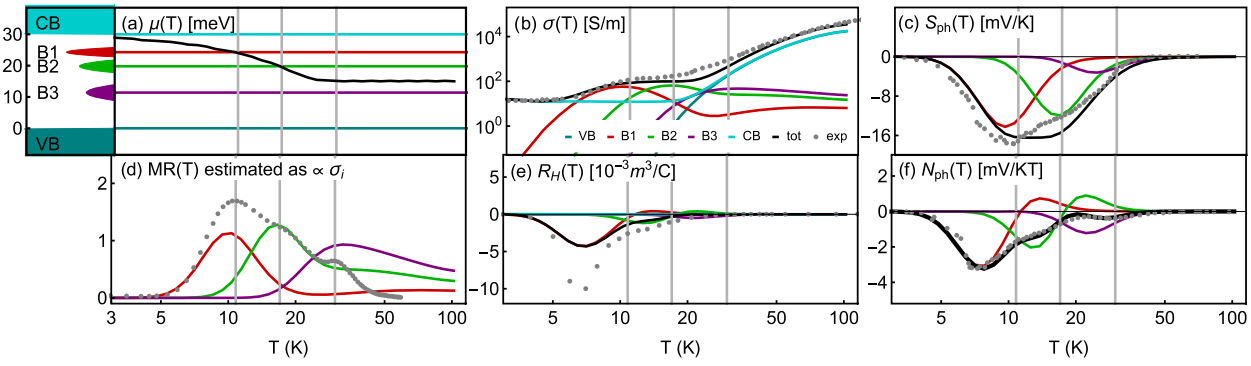

FIG. 2 (color online). Same as Fig. 1 but for three in-gap states: $E_i = 11.4$, 19.8, 24.3 meV. The (gray) vertical lines are guides to the eye indicating maxima in the MR. For details of the fitting procedure see the text and the Supplemental Material [18].

We find the momentum transfer to the electrons—that is needed to justify the large S—to be only ~0.5% of that dissipated by phonons (for details see the Supplemental Material [18]), which is very realistic. Indeed the experimental thermal conductivity is characterized by phonon-crystal boundary scatterings [8], supporting such a small momentum transfer. Consequently, our results show that a large phonon-drag thermopower need not produce temperature characteristics in the thermal conductivity. That a minute transfer of phonon momentum has such a big impact on charge carriers is explained by the large ratio of masses of ions and electrons.

In the Nernst coefficient, the proposed phonon-coupling to the density of in-gap states circumvents Sondheimer cancellation [34], without requiring multiband effects. Previously, it had been proposed that a strongly energy-dependent scattering rate $\tau(\varepsilon)$ causes the colossal Nernst signal [14]. Indeed, we can assume an *effective*, purely electronic picture with a scattering rate $\tau(\varepsilon) \propto \varepsilon^r$, where the exponent is determined by $r = -e/k_B \times N/(R_H\sigma)$. This yields, in our phonon-drag formalism, a large exponent $r = -(\hbar/k_B)\alpha = -229.2$, in reasonable agreement with Ref. [14].

Origin of in-gap states.—We now investigate the possible origin of the in-gap states. The number of states has to be low compared to the weight of the bottom of the conduction band, or the chemical potential will not be able to cross them. Moreover, the in-gap bandwidth must be small compared to the intrinsic charge gap. This suggests the states to stem from local defects. The strong reaction to magnetic fields (MR) then points towards Fe impurities. Using density functional theory calculations, we have modeled the behavior of $FeSb_2$ with different defects and impurities. We find that substituting Fe on Sb sites, i.e., $Fe_{1+x}Sb_{2-x}$, agrees best with the picture proposed above. Our estimate for the minimal defect concentration (see above) translates to $x \approx 4.5 \times 10^{-5}$ [18]. Simulating the effect of iron defects, we show in Fig. 3 the paramagnetic band structure of $Fe_{25}Sb_{47}$ (i.e., $x \approx 0.04$) [35]. Indeed two impurity bands appear close to the conduction states. Moreover, the doping coming from the defect pins the chemical potential (at $T = 0$) to the bottom of the conduction band, in extremely good agreement with the scenario proposed above. This finding is supported by the binary Fe-Sb phase diagram [36] that may suggest Fe richness, and a recent experiment demonstrating that even the smallest iron concentrations in $Ru_{1-x}Fe_xSb_2$ causes the appearance of the low temperature characteristics of $FeSb_2$ [13]. Further support comes from recent magnetic resonance experiments [37] that advocate localized $S = 1/2$ in-gap states slightly below the conduction bands. The presence of Fe defects with localized states entails a Curie-like contribution to the magnetic susceptibility, which can be estimated as follows: Curie's law reads $\chi = x\mu_0 N_A \mu_{\text{eff}}^2/(12\pi T)$, with the vacuum permeability μ_0, Avogadro's constant N_A, an effective local moment $\mu_{\text{eff}} = g_S\sqrt{S(S+1)}\mu_B$, with gyromagnetic factor $g_S = 2$ and Bohr magneton μ_B. Using the experimentally suggested $S = 1/2$ spin state [37] and the minimal defect concentration x yields $\chi T = 5 \times 10^{-6}$ emu K/mol. This is consistent with experiment, witnessing a low temperature upturn in the susceptibility for most samples, with a magnitude smaller than 5×10^{-5} emu/mol [6,7,9,10,38–40] for all accessed temperatures.

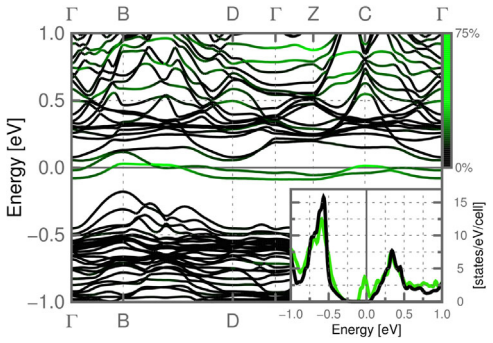

FIG. 3 (color online). Band structure of $Fe_{25}Sb_{47}$, mimicking $Fe_{1+x}Sb_{2-x}$. Hues of green indicate orbital admixtures originating from the extra iron atom. Inset: density of states of pure (black) and Fe-rich (green) $FeSb_2$.

Summary.—Purely electronic transport properties of $FeSb_2$, like the conductivity and the Hall coefficient, can be described with impressive accuracy from an effective one-particle electronic structure [41] when taking into account the influence of defect-derived in-gap states. Using *ab initio* band theory, we identified surplus iron, $Fe_{1+x}Sb_{2-x}$, as the likely origin of these states. Our work provides a unified picture: there is only one independent transport property, from which the features of all five other response functions are determined in a one-to-one correspondence. Finally, we have pinpointed the phonon-drag associated with the density of in-gap states as the microscopic origin of the hitherto elusive colossal thermoelectricity in $FeSb_2$. Our findings have important consequences for the quest of reducing the thermal conduction. Selective phonon engineering, e.g., by nanostructuring [3,46], needs to take care that the phonon drag mechanism survives. Our scenario might also be relevant for understanding other narrow-gap semiconductors, such as $CrSb_2$ [47] or $FeGa_3$ [48,49].

We thank S. Bühler-Paschen, Y. Nomura, C. Petrovic, A. Prokofiev, F. Steglich, P. Sun, and V. Zlatic for fruitful discussions, and P. Sun for providing the experimental data of Ref. [14]. This work has been supported in part by the European Research Council under the European Union's Seventh Framework Program (FP/2007-2013)/ERC through Grant Agreement No. 306447, and COST Action MP1306 EUSpec (J. M. T.). Numerical calculations have been achieved in part using the Vienna Scientific Cluster (VSC).

*Corresponding author.
marco.battiato@ifp.tuwien.ac.at

[1] V. Zlatić and R. Monnier, *Modern Theory of Thermoelectricity* (Oxford University Press, New York, 2014).
[2] G. J. Snyder and E. S. Toberer, Nat. Mater. **7**, 105 (2008).
[3] J. P. Heremans, M. S. Dresselhaus, L. E. Bell, and D. T. Morelli, Nat. Nanotechnol. **8**, 471 (2013).
[4] S. Donsa, S. Andergassen, and K. Held, Phys. Rev. B **89**, 125103 (2014).
[5] S. Cho, S. D. Kang, W. Kim, E.-S. Lee, S.-J. Woo, K.-J. Kong, I. Kim, H.-D. Kim, T. Zhang, J. A. Stroscio, Y.-H. Kim, and H.-K. Lyeo, Nat. Mater. **12**, 913 (2013).
[6] C. Petrovic, J. W. Kim, S. L. Bud'ko, A. I. Goldman, P. C. Canfield, W. Choe, and G. J. Miller, Phys. Rev. B **67**, 155205 (2003).
[7] C. Petrovic, Y. Lee, T. Vogt, N. D. Lazarov, S. L. Bud'ko, and P. C. Canfield, Phys. Rev. B **72**, 045103 (2005).
[8] A. Bentien, S. Johnsen, G. K. H. Madsen, B. B. Iversen, and F. Steglich, Europhys. Lett. **80**, 17008 (2007).
[9] P. Sun, N. Oeschler, S. Johnsen, B. B. Iversen, and F. Steglich, Dalton Trans. **39**, 1012 (2010).
[10] P. Sun, N. Oeschler, S. Johnsen, B. B. Iversen, and F. Steglich, Appl. Phys. Express **2**, 091102 (2009).
[11] Q. Jie, R. Hu, E. Bozin, A. Llobet, I. Zaliznyak, C. Petrovic, and Q. Li, Phys. Rev. B **86**, 115121 (2012).
[12] P. Sun, N. Oeschler, S. Johnsen, B. B. Iversen, and F. Steglich, Phys. Rev. B **79**, 153308 (2009).
[13] M. K. Fuccillo, Q. D. Gibson, M. N. Ali, L. M. Schoop, and R. J. Cava, APL Mater. **1**, 062102 (2013).
[14] P. Sun, W. Xu, J. M. Tomczak, G. Kotliar, M. Søndergaard, B. B. Iversen, and F. Steglich, Phys. Rev. B **88**, 245203 (2013).
[15] J. M. Tomczak, K. Haule, T. Miyake, A. Georges, and G. Kotliar, Phys. Rev. B **82**, 085104 (2010).
[16] M. Pokharel, H. Zhao, K. Lukas, Z. Ren, C. Opeil, and B. Mihaila, MRS Commun. **3**, 31 (2013).
[17] K. Behnia, J. Phys. Condens. Matter **21**, 113101 (2009).
[18] See Supplemental Material at http://link.aps.org/supplemental/10.1103/PhysRevLett.114.236603 for details of the methodology, which includes Refs. [19–30].
[19] J. M. Ziman, *Electrons and Phonons: The Theory of Transport Phenomena in Solids* (Oxford Classic Texts in the Physical Sciences, New York, 2001).
[20] G. Kresse and J. Hafner, Phys. Rev. B **47**, 558 (1993).
[21] F. Tran and P. Blaha, Phys. Rev. Lett. **102**, 226401 (2009).
[22] P. Blaha, K. Schwarz, G.-K.-H. Madsen, D. Kvasnicka, and J. Luitz, *Wien2k, An Augmented Plane Wave Plus Local Orbitals Program for Calculating Crystal Properties* (Vienna University of Technology, Austria, 2001), ISBN 3-9501031-1-2.
[23] G. Madsen, A. Bentien, S. Johnsen, and B. Iversenm, in *25th International Conference on Thermoelectrics, ICT '06.* (2006), p. 579.
[24] A. V. Lukoyanov, V. V. Mazurenko, V. I. Anisimov, M. Sigrist, and T. M. Rice, Eur. Phys. J. B **53**, 205 (2006).
[25] M. S. Diakhate, R. P. Hermann, A. Möchel, I. Sergueev, M. Søndergaard, M. Christensen, and M. J. Verstraete, Phys. Rev. B **84**, 125210 (2011).
[26] L. Hedin, Phys. Rev. **139**, A796 (1965).
[27] S. Biermann, F. Aryasetiawan, and A. Georges, Phys. Rev. Lett. **90**, 086402 (2003).
[28] A. Toschi, G. Rohringer, A. Katanin, and K. Held, Ann. Phys. **523**, 698 (2011).
[29] A. van Roekeghem, T. Ayral, J. M. Tomczak, M. Casula, N. Xu, H. Ding, M. Ferrero, O. Parcollet, H. Jiang, and S. Biermann, Phys. Rev. Lett. **113**, 266403 (2014).
[30] J. M. Tomczak, J. Phys. Conf. Ser. **592**, 012055 (2015).
[31] H. Takahashi, R. Okazaki, I. Terasaki, and Y. Yasui, Phys. Rev. B **88**, 165205 (2013).
[32] The remaining small quantitative discrepancies can be shown to mainly derive from modeling the highly anisotropic $FeSb_2$ [8–11] as isotropic.
[33] We note that a change in τ by 1 order of magnitude yields only a factor of 3 on the bandwidths W_i. Since the latter are constrained by the size of the fundamental gap $\Delta \sim 30$ meV, we belief our choice to be reasonable.
[34] Y. Wang, Z. A. Xu, T. Kakeshita, S. Uchida, S. Ono, Y. Ando, and N. P. Ong, Phys. Rev. B **64**, 224519 (2001).
[35] Describing the gap in $FeSb_2$ requires exchange effects beyond standard band theory [15]. Here we use the modified Becke-Johnson exchange potential to mimic this physics; see Supplemental Material [18]. Also note that a ferromagnetic solution exists, which, however, lies higher in energy.
[36] K. W. Richter and H. Ipser, J. Alloys Compd. **247**, 247 (1997).
[37] A. Gippius, M. Baenitz, K. Okhotnikov, S. Johnsen, B. Iversen, and A. Shevelkov, Appl. Magn. Reson. **45**, 1237 (2014).
[38] R. Hu, V. F. Mitrović, and C. Petrovic, Phys. Rev. B **74**, 195130 (2006).
[39] T. Koyama, Y. Fukui, Y. Muro, T. Nagao, H. Nakamura, and T. Kohara, Phys. Rev. B **76**, 073203 (2007).
[40] I. A. Zaliznyak, A. T. Savici, V. O. Garlea, R. Hu, and C. Petrovic, Phys. Rev. B **83**, 184414 (2011).
[41] This suggests that for $T \lesssim 100$ K electronic correlations renormalize but do not invalidate the band picture. Yet, for $T \gtrsim 100$ K $FeSb_2$ metallizes [42] although $T \ll \Delta$. A similar effect has recently been explained for FeSi [43,44] (see also Ref. [45]), advocating strong many-body effects for $T \gtrsim 100$ K also in $FeSb_2$.
[42] A. Perucchi, L. Degiorgi, R. Hu, C. Petrovic, and V. F. Mitrovic, Eur. Phys. J. B **54**, 175 (2006).
[43] J. M. Tomczak, K. Haule, and G. Kotliar, Proc. Natl. Acad. Sci. U.S.A. **109**, 3243 (2012).
[44] J. M. Tomczak, K. Haule, and G. Kotliar, in *New Materials for Thermoelectric Applications: Theory and Experiment*, NATO Science for Peace and Security Series B: Physics and Biophysics, edited by V. Zlatić and A. Hewson (Springer, Netherlands, 2013), p. 45.
[45] O. Delaire, K. Marty, M. B. Stone, P. R. C. Kent, M. S. Lucas, D. L. Abernathy, D. Mandrus, and B. C. Sales, Proc. Natl. Acad. Sci. U.S.A. **108**, 4725 (2011).
[46] Y. Dubi and M. Di Ventra, Rev. Mod. Phys. **83**, 131 (2011).
[47] B. C. Sales, A. F. May, M. A. McGuire, M. B. Stone, D. J. Singh, and D. Mandrus, Phys. Rev. B **86**, 235136 (2012).
[48] M. B. Gamża, J. M. Tomczak, C. Brown, A. Puri, G. Kotliar, and M. C. Aronson, Phys. Rev. B **89**, 195102 (2014).
[49] M. Wagner-Reetz, D. Kasinathan, W. Schnelle, R. Cardoso-Gil, H. Rosner, Y. Grin, and P. Gille, Phys. Rev. B **90**, 195206 (2014).